J. Fluid Mech. (1978), *vol.* 89, *part* 1, *pp.* 33–47
Printed in Great Britain

Flow around a circular cylinder near a plane boundary

By P. W. BEARMAN
Department of Aeronautics, Imperial College, London
AND M. M. ZDRAVKOVICH
Department of Aeronautical and Mechanical Engineering,
University of Salford, England

(Received 21 November 1977 and in revised form 5 May 1978)

The flow around a circular cylinder placed at various heights above a plane boundary has been investigated experimentally. The cylinder spanned the test section of a wind tunnel and was aligned with its axis parallel to a long plate and normal to the free stream. It was placed 36 diameters downstream of the leading edge of the plate and its height above the plate was varied from zero, the cylinder lying on the surface, to 3·5 cylinder diameters. The thickness of the turbulent boundary layer on the plate at the cylinder position, but with it removed from the tunnel, was equal to 0·8 of the cylinder diameter. Distributions of mean pressure around the cylinder and along the plate were measured at a Reynolds number, based on cylinder diameter, of $4{\cdot}5 \times 10^4$. Spectral analysis of hot-wire signals demonstrated that regular vortex shedding was suppressed for all gaps less than about 0·3 cylinder diameters. For gaps greater than 0·3 the Strouhal number was found to be remarkably constant and the only influence of the plate on vortex shedding was to make it a more highly tuned process as the gap was reduced. Flow-visualization experiments in a smoke tunnel revealed the wake structure at various gap-to-diameter ratios.

1. Introduction

Apart from the aerofoil few shapes have received as much attention from the fluid dynamicist as the circular cylinder. Nevertheless, understanding of the flow around a circular cylinder near to a plane boundary remains limited. This problem is of fundamental interest as well as being important in many engineering applications. We can expect the plane boundary to influence the flow in two distinct ways: first as a solid boundary inhibiting normal velocities and second as a surface along which a boundary layer grows. In some applications, such as the design of pipelines, the cylinder may be totally immersed in a thick boundary layer. In this paper we have concentrated on thin boundary layers, i.e. boundary layers thinner than the diameter of the cylinder.

There is an equivalence in potential flow theory between the flow around a cylinder near to a wall and the flow around two cylinders in a side-by-side arrangement. In a real flow a boundary layer will grow along the wall and also the flows about the two cylinders may not always be mirror images of each other. However this does not completely invalidate the analogy. Depending on the ratio of the gap $2G$ between the two cylinders to the cylinder diameter D, Bearman & Wadcock (1973), and later Quadflieg (1977), identified four distinct flow regimes around two circular cylinders in a side-by-side arrangement (see also the review by Zdravkovich 1977). They found

that for G/D greater than about 2 the two cylinders shed vortices independently, whereas when G/D was between roughly 0·5 and 2 the shedding of vortices from one cylinder was the mirror image of the shedding from the other. An unstable flow regime exists for G/D between 0·5 and 0·05 with the flow in the gap randomly biased towards one cylinder and vortex shedding not clearly defined. When G/D was less than about 0·05 the two cylinders behaved as a single body and only one vortex street was formed. They found a mean repulsive force acting between the two cylinders for all values of G/D examined. Roshko, Steinolfson & Chattoorgoon (1975) have observed similar behaviour on two cylinders of triangular cross-section.

Assuming our analogy to hold, we can make some predictions about the flow around a cylinder near a wall. So long as the boundary layer along the wall is thin, compared with D, we expect, for G/D greater than about 0·5, the cylinder to shed a strong and regular vortex street and that there should be a mean force on the cylinder directed away from the wall. The analogy cannot hold when the cylinder is touching the wall because the wall acts like a splitter plate between the cylinder and its image to inhibit any regular vortex shedding. Also when the cylinder is close to or touching the wall there will be separations of the wall boundary layer upstream and downstream of the cylinder. If a fixed impermeable ground board is used to represent the wall it is impossible to eliminate the influence of the upstream boundary layer. The presence of a cylinder will induce pressure gradients on the ground such that the boundary-layer displacement thickness δ^* may grow very rapidly with x. Although the boundary layer can be thinned, such that δ^* is small, it will still possess non-zero values of $d\delta^*/dx$, $d^2\delta^*/dx^2$, etc. The effect of an upstream boundary-layer separation or a rapid growth of δ^* will be to induce an inclination of the flow approaching the cylinder additional to that imposed by the 'image' of the cylinder in the ground. Again this should lead to a component of the total mean force on the cylinder acting in the direction away from the wall.

Qualitative observations of the flow around a circular cylinder near to a wall have been reported by Taneda (1965). His cylinder was towed in a water tank close to one of the walls and thus he eliminated the upstream wall boundary layer. Taneda's work was carried out at a Reynolds number of 170 and he presented flow-visualization photographs taken at $G/D = 0{\cdot}1$ and 0·6. At $G/D = 0{\cdot}6$ a strong regular street of vortices was observed whereas at $G/D = 0{\cdot}1$ only a single row of vortices was seen. Taneda commented that, when G/D was sufficiently small that only a single row of vortices was formed, the wavelength of the vortices increased with downstream distance and after a few wavelengths the wake became unstable and broke down.

Roshko *et al.* (1975) measured lift and drag coefficients on both a circular and a triangular cross-sectioned cylinder near a wall at values of G/D from 0 to 6. Their experiments were carried out in air at a Reynolds number of 2×10^4 and the thickness of the wall boundary layer, in the absence of the cylinder, was about $0{\cdot}5D$. They found that far from the wall the drag coefficient C_D of the circular cylinder was about 1·2 and that it increased slightly as G/D was reduced to about 0·6. With further reductions in G/D, C_D decreased rapidly down to a value of 0·8 when the cylinder was touching the wall. The decrease in drag was attributed to the interference of the wall with vortex shedding and the immersion of the cylinder in the lower energy wall-boundary-layer flow. Also Göktun (1975) has recently investigated the flow around a circular cylinder near to a wall at Reynolds numbers between $0{\cdot}9 \times 10^5$ and $2{\cdot}5 \times 10^5$. In his

experiments the wall was represented by a plate parallel with the flow and the cylinder was positioned at 2, 4 and 8 diameters downstream of the leading edge. At these three stations, for a given G/D, he found no differences in the values of the lift and drag evaluated from measurements of pressure distributions. The thickness of the boundary layer in the absence of the cylinder was not measured but it would have been thin and presumably laminar. Göktun found a minimum drag at $G/D = 0$, similar to that measured by Roshko *et al.* (1975), but the maximum value of C_D was between 1·4 and 1·5, at $G/D = 0{\cdot}5$. He also found a slight increase in the Strouhal number S as the cylinder was moved in from the free stream towards the wall. The Strouhal number increased from 0·198 in the free stream to 0·206 at $G/D = 0{\cdot}5$.

Summing up what has been done to date, it is evident that at least three important aspects of the wall interference problem have not been examined.

(i) How does vortex shedding cease as the wall is approached? Does it stop at some critical value of G/D or does it slowly diminish?

(ii) What effect does a turbulent boundary layer along the wall have on the phenomenon? This aspect is relevant for most practical applications.

(iii) How does the flow change along the wall during the various phases of the interference with the cylinder? This question is relevant for pipelines laid along a sea or river bed, where scouring due to this flow could change considerably the gap between the pipe and the bed and also alter the shape of the bed itself.

2. Experimental arrangement

The experiments were performed in the Department of Aeronautics at Imperial College. A wind tunnel of the closed-return type with a test section 1 m high, 0·61 m wide and about 3 m long was used. The free-stream turbulence level was less than 0·2 % at the top speed of 38 m/s. An aluminium cylinder of diameter 1·9 cm spanned the wind tunnel horizontally, thus having a length-to-diameter ratio of 32. The cylinder was pressure tapped at the mid-span and by rotating it pressure measurements could be made at any angular position.

The working section was divided by a horizontal partition plate situated in the middle of the tunnel. The plate was 1 m long and 10 mm thick and had a rounded leading edge. A small adjustable flap was fitted along the trailing edge of the plate to correct any flow asymmetry near the leading edge caused by the presence of the cylinder. The optimum flap position was found for each run by matching pressures recorded on tappings located on the top and bottom of the plate 5 cm from the leading edge. A trip wire of diameter 1 mm was attached across the plate 14 cm from the leading edge. The cylinder was situated 0·68 m, or 36 cylinder diameters, from the leading edge. The partition plate was pressure tapped at the mid-span in the region beneath the cylinder. A central tapping was fitted under the axis of the cylinder and the rest were positioned at $\frac{1}{4}$, $\frac{1}{2}$, 1, 2 and 3 cylinder diameters upstream and downstream of it. The gap between the cylinder and the plate was varied over the range 0–3·5 cylinder diameters. At all values of G/D checks were made to ensure that the gap remained constant across the span.

A Disa constant-temperature hot-wire anemometer was used to measure velocity fluctuations generated by the cylinder. The anemometer output was recorded on analog tape for later conversion to digital data and subsequent calculation of power

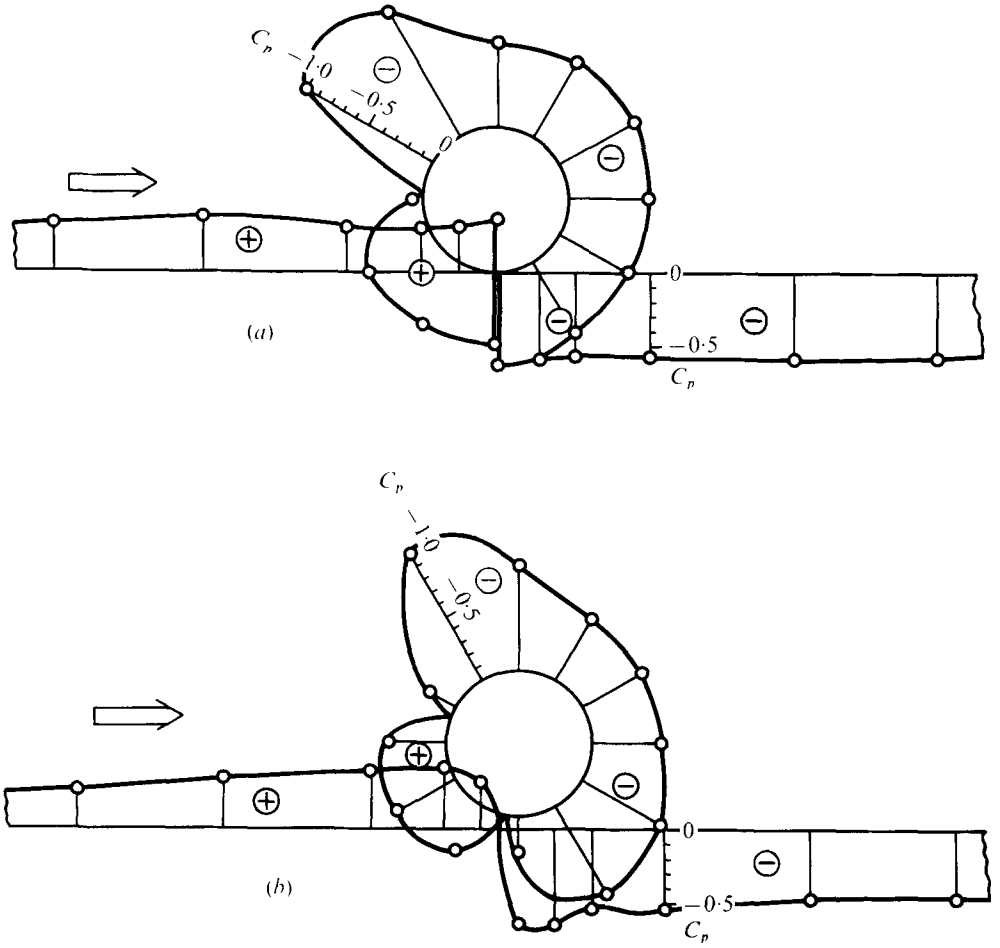

FIGURE 1. Pressure distribution around the cylinder and along the plate. (*a*) $G/D = 0$; (*b*) $G/D = 0{\cdot}1$.

spectra on a CDC 6400 computer. Further details of the computation techniques are given by Davies (1974).

Flow-visualization experiments were conducted in a smoke tunnel with a working section 0·6 m high and only 5 cm wide. A cylinder 5 cm in diameter was used in order to generate a flow with a cylinder Reynolds number the same as that in the main wind tunnel experiments. The cylinder was positioned 6 diameters downstream of the leading edge of the plate and no trip wire was attached to the plate. In the main wind tunnel experiments flow was visualized by using the surface oil-flow technique.

3. Experimental results

The experiments were conducted at two Reynolds numbers based on the cylinder diameter: $Re = 2{\cdot}5 \times 10^4$ and $4{\cdot}8 \times 10^4$. This is within the range where the drag coefficient and the Strouhal number of a circular cylinder are relatively independent of the Reynolds number. Pressure measurements were carried out mainly at $Re = 4{\cdot}8 \times 10^4$

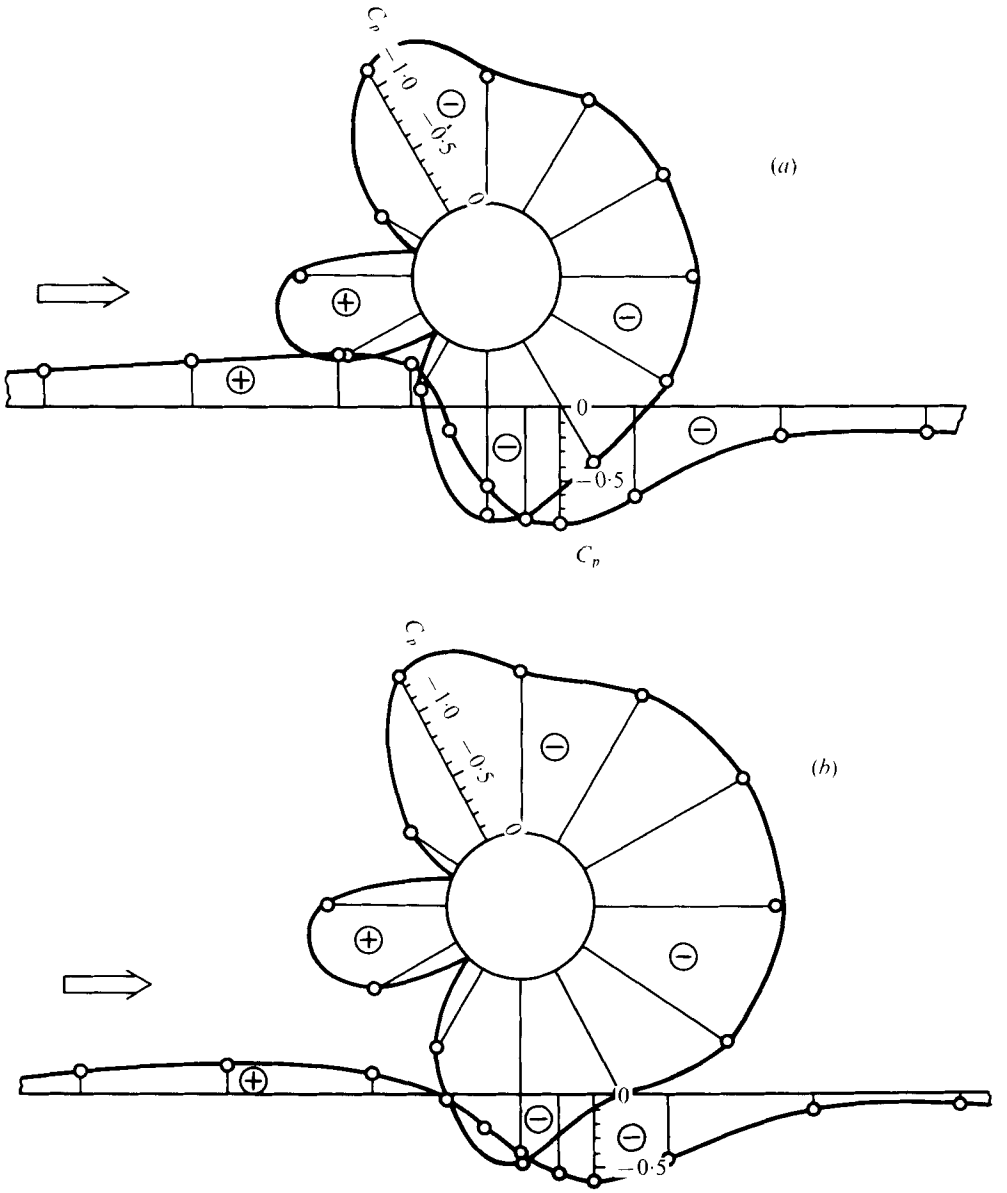

FIGURE 2. Pressure distribution around the cylinder and along the plate. (*a*) $G/D = 0{\cdot}4$; (*b*) $G/D = 0{\cdot}8$.

but it was decided to conduct all hot-wire surveys at $Re = 2{\cdot}5 \times 10^4$ because vibrations of the hot-wire support were experienced at the higher Reynolds number. The thickness of the turbulent boundary layer on the wall at the position of the cylinder, but with it removed from the tunnel, was found to be about 1·5 cm, or $0{\cdot}8D$.

3.1. *Pressure distributions*

Time-averaged pressure distributions around the cylinder and along the plate are shown in figures 1–3. Pressures are presented non-dimensionally in the form of

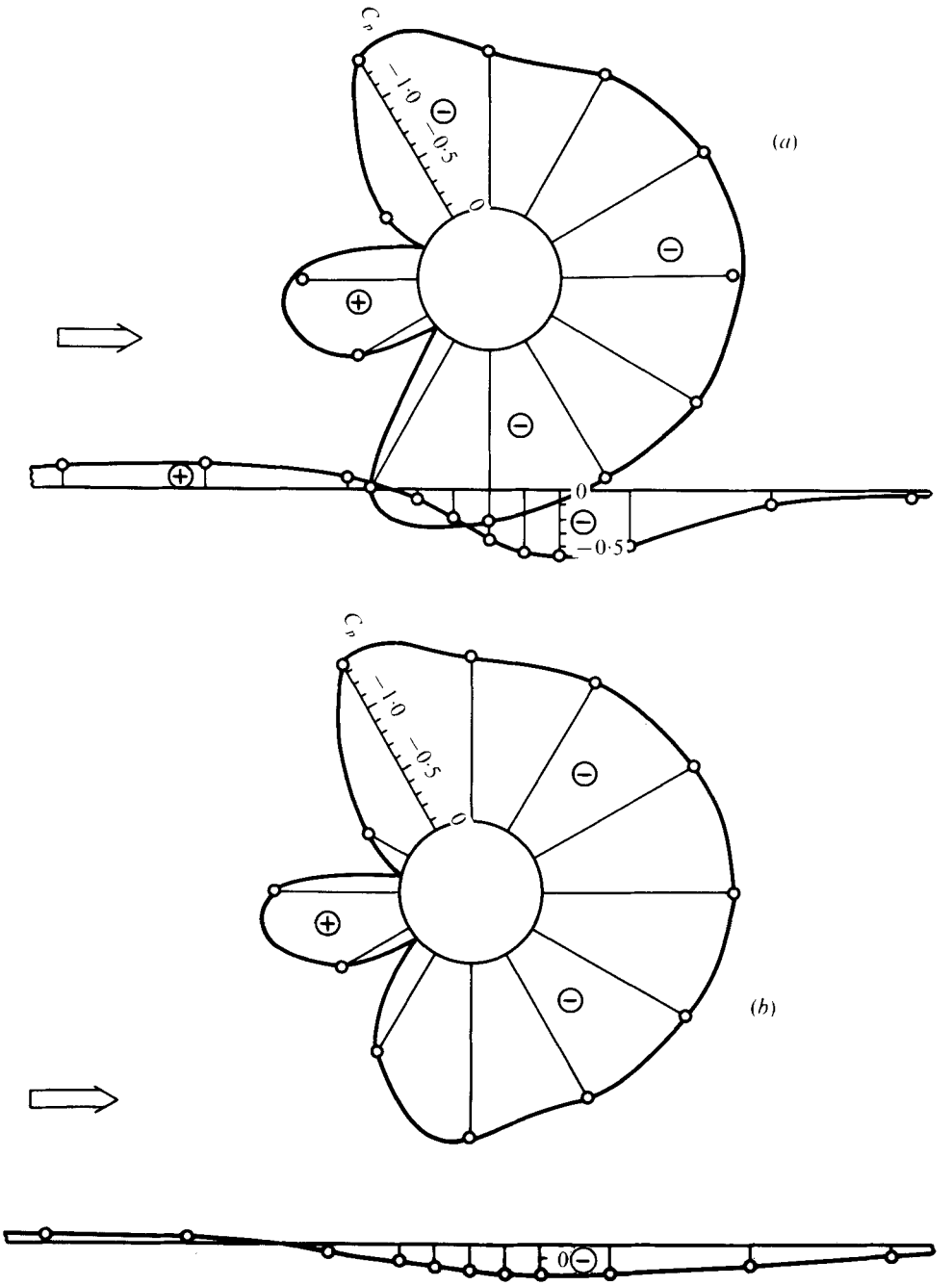

FIGURE 3. Pressure distribution around the cylinder and along the plate. (*a*) $G/D = 1$; (*b*) $G/D = 2{\cdot}0$.

pressure coefficients C_p; the reference velocity and static pressure are taken as those near the leading edge of the plate. The cylinder occupied just under 2 % of the total height of the tunnel but no attempt was made to apply a conventional blockage correction.

Figure 1 shows two asymmetric pressure distributions around the cylinder. The distribution for the cylinder lying on the plate is plotted in figure 1 (*a*) and at the point of contact a discontinuity in pressure is evident on both the cylinder and the plate. Within the span of the pressure tappings on the plate, $3D$ upstream and downstream of the cylinder axis, the upstream separated region has an almost constant positive C_p and the downstream separated region displays a constant negative C_p. Figure 1 (*b*) reveals the effects of a gap flow on the pressure distribution on the plate for $G/D = 0{\cdot}1$. There is a rapid fall in pressure under the cylinder and the minimum C_p is recorded just behind the gap.

Figure 2 shows the pressure distributions for $G/D = 0{\cdot}4$ and $0{\cdot}8$ and it can be seen that the pressure distributions on the cylinder are nearly symmetric about the front stagnation point. The base-pressure coefficient C_{pb} becomes markedly more negative in this range of G/D. Unlike the pressure distribution shown in figure 1 (*b*), there is a continuous recovery of the pressure along the plate after the minimum C_p and the magnitude of this minimum pressure decreases as G/D is increased. Pressure distributions at $G/D = 1{\cdot}0$ and $2{\cdot}0$ are shown in figure 3. The base pressure is observed to change very little above $G/D = 1{\cdot}0$. As G/D is increased the pressure distribution assumes a symmetrical form with the axis of symmetry approaching the free-stream direction. The pressure distributions around the cylinder, for all values of G/D, are in general agreement with Göktun's (1975) measurements.

Figure 4 shows the variation of C_{pb} with the gap-to-diameter ratio, C_{pb} being measured at the downstream end of a diameter parallel to the plane boundary. Measurements of C_{pb} for $Re = 2{\cdot}5 \times 10^4$ are also shown in figure 4, where it can be seen that Reynolds number had a small influence very close to the wall.

Figure 5 shows the position along the plate and magnitude of the negative peak in C_p for various G/D ratios. When the cylinder is touching the plate the pressure minimum is at the point of contact, i.e. $X_{C_{p\,\min}} = 0$. In the range of strong interference when the cylinder is near the wall, the peak becomes more pronounced and its position moves downstream. At $G/D = 0{\cdot}4$ the pressure peak reaches its maximum magnitude and occurs underneath the rear of the cylinder, at $0{\cdot}5D$. The peak remains at this point for all $G/D > 0{\cdot}4$. Thus, as far as the flow along the plate is concerned, there are two distinct regimes and the gaps in the curves shown in figure 5 indicate that the precise value of G/D at which this change occurs was not found. It will be shown in the next section that in the lower range of G/D there are two separation bubbles attached to the plate, whereas in the upper range there are none.

3.2. *Flow visualization*

The first objective of the flow-visualization experiments was to establish the existence of separation bubbles along the plate at various gap-to-diameter ratios. At $G/D = 0$ large separation regions were found on the plate upstream and downstream of the cylinder. At small gaps separation bubbles again formed on the plate upstream and downstream of the cylinder but the flow in the gap ensured that these were not attached

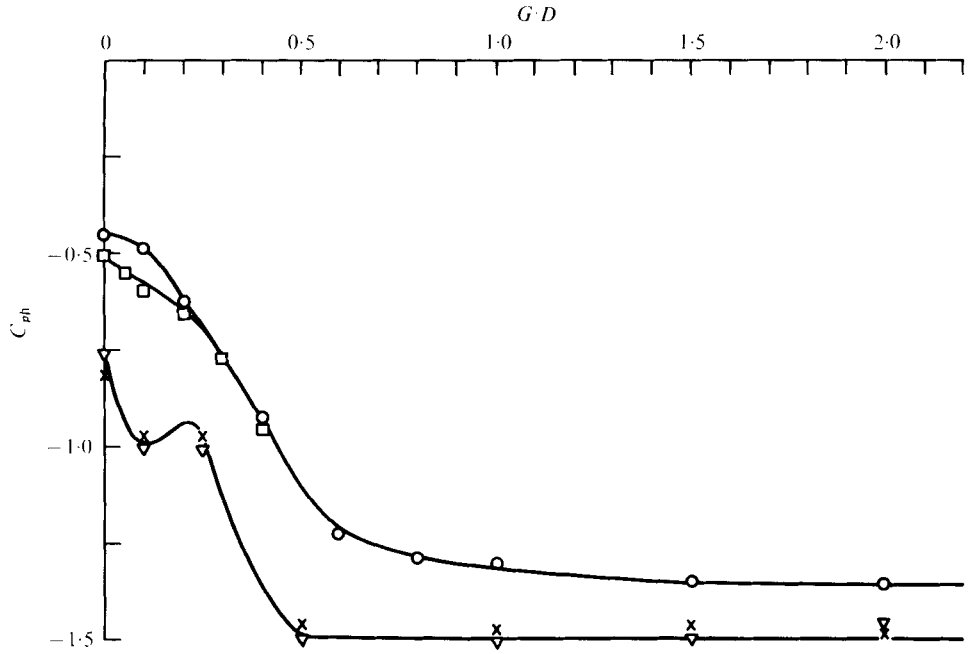

FIGURE 4. Base-pressure coefficient against the gap ratio.

	Re	*L/D*	*δ/D*	Source
□	$2{\cdot}5 \times 10^4$	36	0·8	Our tests
○	$4{\cdot}8 \times 10^4$	36	0·8	Our tests
×	9×10^4	4	0·2	Göktun
▽	$1{\cdot}5 \times 10^4$	8	0·2	Göktun

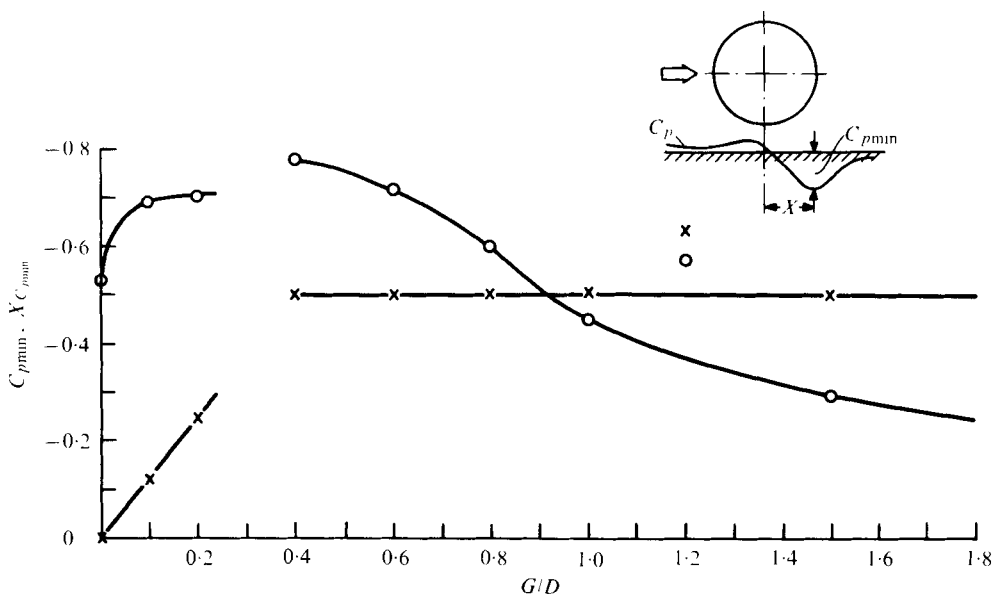

FIGURE 5. Minimum pressure coefficient on the plate.
○, C_{pmin}; ×, position of C_{pmin}.

to the cylinder. A thin separation bubble was just visible upstream of the cylinder for $G/D = 0{\cdot}4$ but by $G/D = 0{\cdot}6$ all bubbles had disappeared.

A cylinder model was made with a small slot running along the back through which smoke could enter the wake. The Reynolds number for the experiments carried out in the smoke tunnel was the same as that used for the hot-wire measurements in the main wind tunnel. Figures 6 and 7 (plates 1 and 2) show photographs of the flow with a combination of parallel smoke filaments and smoke ejected through the slot in the cylinder. Figure 6(*a*) (plate 1) reveals the flow pattern for $G/D = 0$ and figure 6(*b*) (plate 1) shows the flow for $G/D = 0{\cdot}2$. In these two pictures the wake flow appears similar although in the second there is a flow between the cylinder and the wall and the geometry of the upstream separation bubble is different. The flow pattern for $G/D = 0{\cdot}4$ is shown in figure 6(*c*) (plate 1), where one smoke filament is seen being entrained into the wake after having passed between the cylinder and the wall. The greater curvature of the smoke filaments above the wake for $G/D = 0{\cdot}4$ suggests a shorter recirculation region behind the cylinder and a lower base pressure compared with the cases with smaller gaps. This is in agreement with the base-pressure measurements plotted in figure 4. Figure 7 (plate 2) shows visualizations of the wake for $G/D = 0{\cdot}8$, $1{\cdot}2$ and $2{\cdot}0$ and for each gap vortex shedding is clearly visible behind the cylinder. At these larger gaps the unsteady flow around the cylinder appears to be little affected by the presence of the wall.

It should be noted that the smoke-tunnel work was not carried out under identical conditions to those of the wind-tunnel experiments. Although the cylinder Reynolds number was the same this was achieved at the expense of a thinner approaching boundary layer on the plate and with a cylinder length-to-diameter ratio of only 1. Further, there was the possibility that the flow of smoke ejected through the slot in the back of the cylinder could have altered the flow pattern. However this flow was kept as small as possible and did not appear to modify the near-wake structure. It is thought that the photographs of the flow at the mid-span give a qualitative picture which is not too remote from that in the wind-tunnel experiments.

3.3. *Measurements of vortex shedding frequency*

The interference between the cylinder and the plane boundary may be either weak with only a small effect on the frequency of vortex shedding or strong enough to inhibit shedding either on the gap side or on both sides of the cylinder. Systematic analyses of velocity fluctuations on both sides of the wake at various G/D ratios have been carried out and initially measurements were made behind the cylinder in the absence of the plate. Power spectra taken outside the wake with the plate removed from the tunnel showed typically a pronounced peak at the vortex shedding frequency with a sharp fall-off in spectral density above the shedding frequency. A broad low frequency hump centred on a frequency about 5% of the shedding frequency and associated with a low frequency modulation of the shedding signal was seen. When the hot wire was moved inside the wake the peak at the shedding frequency was seen to rise from a nearly uniform background turbulence spectrum.

With the plate in position hot-wire signals were recorded for $G/D = 3{\cdot}5$ down to zero. Table 1 gives, for all the G/D ratios tested, the hot-wire position and the frequency of vortex shedding expressed non-dimensionally as a Strouhal number. The signals

No.	G/D	x/D	y/D	St	x/D	y/D	St
1	3.5	1·0	1·5	0·203	1·0	−3·5	0·202
2	2·5	0·9	1·1	0·195	1·0	−2·2	0·194
3	2·0	1·0	1·6	0·215	1·0	−1·4	0·212
4	1·5	—	—	—	1·0	−1·3	0·204
5	0·8	1·0	1·5	0·213	0·5	−0·8	0·208
6	0·6	1·0	1·5	0·203	0·5	−0·8	0·205
7	0·4	1·0	1·4	0·202	0·5	−0·6	0·202
8	0·3	1·0	2·9	0·207	0·5	−0·6	0·206
9	0·2	1·0	1·5	0·190*	0·4	−0·6	(0·035)
10	0·0	2·0	0·8	(0·085)	2·0	−0·3	(0·016)
11	∞	1·0	1·5	0·208	1·0	−1·5	0·204

TABLE 1. Position of hot wire and Strouhal number (estimated from the peak in the power spectrum). x and y measured from the cylinder centre. Entries in parentheses denote a broad low frequency peak, the starred entry a weak shedding peak.

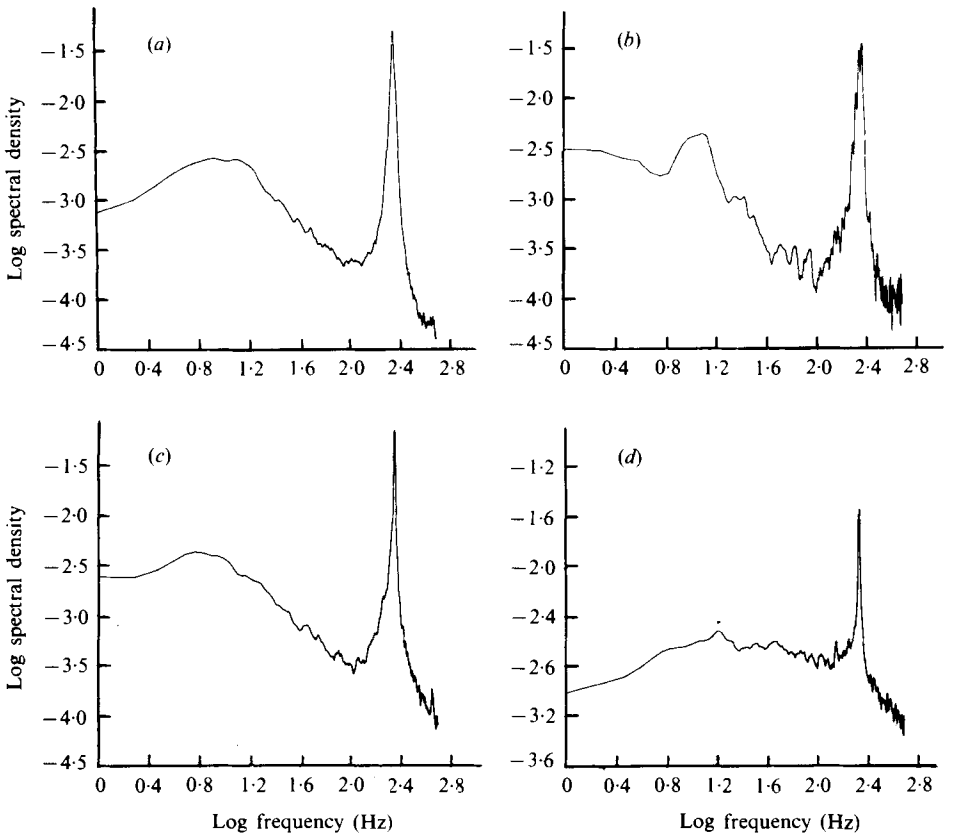

FIGURE 9. Power spectra of hot-wire signals for the cylinder near the plate. (*a*) $G/D = 2{\cdot}0$, upper edge; (*b*) $G/D = 2{\cdot}0$, lower edge; (*c*) $G/D = 0{\cdot}3$, upper edge; (*d*) $G/D = 0{\cdot}3$, lower edge.

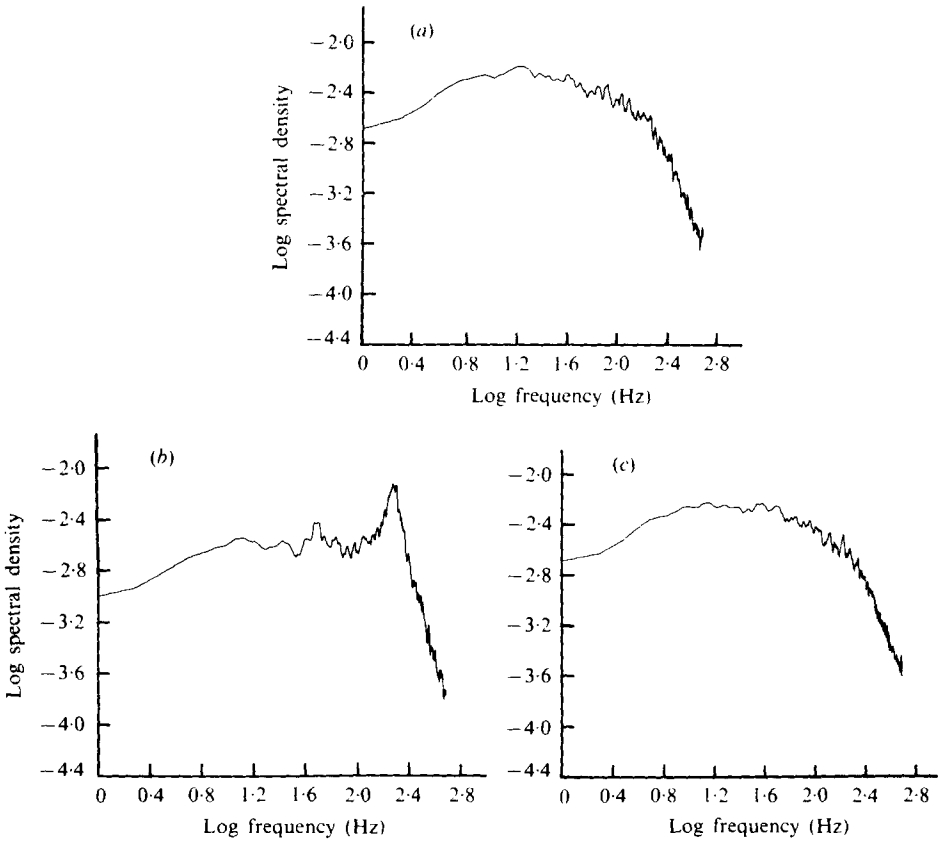

FIGURE 10. Power spectra of hot-wire signals for the cylinder lying on and almost touching the plate. (*a*) $G/D = 0$; (*b*) $G/D = 0{\cdot}2$, upper edge; (*c*) $G/D = 0{\cdot}2$, lower edge.

detected on both the upper and the lower edge of the wake had an obvious predominant frequency for gaps down to $G/D = 0{\cdot}8$. At $G/D = 0{\cdot}8$ there was only a very narrow range of hot-wire positions near the lower edge of the wake on the gap side in which irrotational fluctuations due to vortices could be found. Even then the signals were intermittently turbulent. By $G/D = 0{\cdot}6$ the signal from a hot wire on the gap side 0·5 diameters behind the centre of the cylinder showed turbulence superimposed on a predominant frequency. This feature is illustrated in figure 8(*a*) (plate 3), which shows typical signals detected on the upper and lower sides of the wake for $G/D = 0{\cdot}6$. It appeared that the turbulent shear layer separating from the lower shoulder of the cylinder had merged with the turbulent boundary layer on the plate. Figure 8(*b*) (plate 3) illustrates the development of further irregularities in the signal from the lower edge at $G/D = 0{\cdot}4$, whereas the signal from the upper edge clearly shows vortex shedding. An entirely different picture is revealed for $G/D = 0{\cdot}2$ in figure 8(*c*) (plate 3), where it appears that regularity is lost from the signals above and below the cylinder. Finally, figure 8(*d*) (plate 3) shows a trace for $G/D = 0$ taken at the upper edge of the separated region and no regularity is apparent.

Spectral analysis was performed for all the hot-wire signals over the range of G/D investigated. All the power spectra for gaps from $G/D = 3{\cdot}5$ down to $G/D = 0{\cdot}3$

were remarkably similar. The most surprising feature was that the vortex shedding peak remained at an almost constant Strouhal number as shown in table 1. The absolute value of the peak spectral density changed very little on the upper edge with varying G/D. This was not true on the lower edge, but here the spectra are complicated by variation of the hot-wire position and increasing turbulence level.

Typical examples of power spectra are shown in figure 9. The spectra are presented on a log–log plot; the scale for the power spectral density is arbitrary whereas the frequency scale is in hertz. The first pair of plots shows spectra for $G/D = 2{\cdot}0$ and these were found to be almost identical to the spectra taken without the plate. The second pair of graphs illustrates spectra for the lower limit $G/D = 0{\cdot}3$, where a strong shedding peak was found. Despite the highly turbulent signal detected on the lower edge of the wake, a remarkable peak is seen. The shedding process at $G/D = 0{\cdot}3$ appears to be more highly tuned than that recorded at larger gaps.

An entirely different picture was obtained for $G/D < 0{\cdot}3$. Figure 10 shows that there is no predominant frequency when the cylinder is touching the plate. In order to check whether vortex shedding was merely postponed and appeared further downstream the hot wire was traversed 8 diameters downstream of the cylinder. No regular shedding was observed. Power spectra obtained from signals taken at $G/D = 0{\cdot}2$ are shown in figure 10(*b*) for the upper edge and in figure 10(*c*) for the lower edge. The 'awakening' of vortex shedding is shown in figure 10(*b*), where the small peak is in the right frequency range to assume that it is due to weak and perhaps intermittent bursts of vortex shedding.

4. Discussion of results

It is expected that the flow around a cylinder near to a wall will depend upon the Reynolds number based on the cylinder diameter, the ratio of the gap between the cylinder and the wall to the cylinder diameter and the characteristics of the wall boundary layer. In our experiments, in common with those of Göktun (1975), we have introduced a thin plate into the flow to represent the wall. Göktun placed his cylinder at 2, 4 and 8 cylinder diameters from the leading edge of the plate compared with our distance of 36 diameters. When working with the cylinder very close to the leading edge it is unlikely that the approaching boundary layer can approximate that growing on a flat plate in a zero pressure gradient and under some conditions separation from the leading edge may even occur. Therefore when a plate is used an important variable will be the position of the cylinder relative to the leading edge of the plate.

The tentative analogy between flow around two bluff cylinders in a side-by-side arrangement and flow around a single cylinder near to a wall has been outlined in the introduction. It will be discussed again in the light of our experimental results.

When the cylinder touched the wall there was no regular shedding of vortices, as evidenced by the absence of peaks in the spectra of velocity records. As expected there was no analogy with the two-cylinder case because the wall inhibited the formation of a vortex street and stable separated regions were established upstream and downstream of the cylinder. For small gaps between two cylinders Bearman & Wadcock (1973) found the flow to be biased more towards one cylinder than the other

and that the flow switched between the cylinders at random intervals. Such a bistable, biased flow has not been found in the present tests with a cylinder near a wall.

The flow around a cylinder near a plate has one feature in common with flow around two cylinders in the 'biased' regime: the lack of regular vortex shedding. The peak in all spectra for $G/D < 0{\cdot}3$ was either absent or at least an order of magnitude weaker than that found for $G/D > 0{\cdot}3$. At a Reynolds number of 170 and for $G/D = 0{\cdot}1$ Taneda (1965) observed a single row of vortices. The longitudinal spacing of these vortices was found to increase with downstream distance and they resembled structures observed by Brown & Roshko (1974) in a mixing layer. The lack of a peak in our spectra is no proof that these vortices were absent from our experiment but does indicate that there was no regular vortex street at small gaps. The hot-wire signals presented in figure 8 show a regular frequency emerging as $G/D \rightarrow 0$ of about 5 or 6 times the isolated-cylinder vortex shedding frequency. The origin of this frequency was not investigated but it is thought to be related to the transition waves reported by Bloor (1964).

The pressure distribution around the cylinder for small gaps was characterized by a displacement of the front stagnation point towards the gap. Although the pressure within the separated region was constant there was a lack of symmetry of the distribution about the front stagnation point. Oil flow visualization showed that the separation point on the cylinder nearest to the wall moved as far downstream of the cylinder shoulder as the upper separation point was displaced upstream of the upper shoulder. The same shift in the separation points was observed by Göktun (1975) at higher Reynolds number. He proposed that this shift was caused by the transition from subcritical flow to critical flow around the gap side of the cylinder. This suggestion cannot be accepted in the present experiments, where the Reynolds number is an order of magnitude lower. The shift in the separation position seems to be due simply to the favourable pressure gradient produced by the gap flow between the cylinder and the nearby wall. This favourable pressure gradient is evident from the pressure distributions measured along the plate.

For gaps greater than $G/D \simeq 0{\cdot}5$ there was a close correspondence between the flow about two cylinders and that about one cylinder near a wall. It was in this regime that the flows about two cylinders were mirror images of each other. At gaps less than $G/D = 0{\cdot}5$ (for two cylinders G represents half the distance between the cylinders) the flow about two cylinders broke down into the biased, bistable regime. In the case of a cylinder near to a wall the 'mirrored' type of flow regime was maintained down to $G/D = 0{\cdot}3$. It came as a surprise that the Strouhal number, once established, did not depend on the distance between the cylinder and the wall. Bearman & Wadcock (1973), however, also found that as two cylinders were brought together the Strouhal number remained constant until the onset of the biased flow regime.

It should be emphasized that in our experiments we have not examined the influence of the thickness and upstream history of the boundary layer growing on the wall. If the boundary layer is thick compared with the diameter of the cylinder it seems that the Strouhal number should depend on G/D. A separate study is required to examine the importance of the characteristics of the approaching boundary layer.

Pressure distributions around the cylinder showed that as G/D was reduced there was always a mean force on the cylinder repelling it from the wall. This force falls off very rapidly as the cylinder is moved away from the surface. Roshko *et al.* (1975)

found in their experiments that the non-dimensional normal-force coefficient on a circular cylinder was 0·6 when the cylinder touched the wall whereas at $G/D = 0{\cdot}3$ it drops to 0·16.

Figure 4 shows how the base pressure increases as the ground is approached. Although the base pressure rises rapidly between $G/D = 0{\cdot}6$ and 0·3 the Strouhal number shows no change. This indicates that the strength of the shed vortices, their position of formation or possibly both change as G/D is reduced below about 0·6. A further interesting feature is that the vortex shedding process appears to become more sharply tuned as the gap between the cylinder and the wall is reduced before the shedding disappears at a G/D just less than 0·3. This suggests that a lightly damped cylinder mounted just above a surface could experience vortex-induced oscillations. The base-pressure measurements of Göktun (1975) are also plotted in figure 4, and, apart from a kink in the curve around $G/D = 0{\cdot}25$, the trend is similar to that of the present results. Göktun's base pressures are consistently lower than those reported here but this can probably be attributed to the fact that his cylinder occupied 11 % of the total height of his tunnel and, as in the present experiments, no blockage correction was applied.

5. Conclusions

The interference between the flow around the circular cylinder and the flat plate displayed a number of interesting characteristics. Spectral analysis of hot-wire signals revealed that regular vortex shedding persisted at the same Strouhal number for all gaps down to $G/D = 0{\cdot}3$. As the plate was approached velocity fluctuations, due to the shedding of vortices, became confined to an even narrower band of frequencies. At a point fixed relative to the cylinder the peak power spectral density of the velocity fluctuations hardly changed as the gap was reduced to $G/D = 0{\cdot}3$. For all values of $G/D < 0{\cdot}3$ strong regular vortex shedding was suppressed although in some cases a very weak shedding signal was found near the edge of the cylinder furthest from the plate.

Pressure distributions were measured around the cylinder and along the plate for various G/D ratios. At all the G/D ratios where vortex shedding was suppressed separation bubbles formed on the plate upstream and downstream of the cylinder. When the cylinder was touching the plate the separation bubbles attached themselves to the cylinder. At the value of G/D corresponding to the establishment of strong vortex shedding the suction peak on the plate reached a maximum and was situated half a diameter downstream of the cylinder axis. Further increases in the gap-to-diameter ratio reduced the suction peak on the plate but its position remained fixed. As the cylinder was moved away from the plate the pressure distribution around the cylinder became more symmetric about the front stagnation point and by $G/D = 0{\cdot}4$ it was almost perfectly symmetric. At small gaps the separation point on the side nearest the wall moved downstream of the narrowest point of the gap. The flow remained subcritical and the delayed separation was due to the favourable pressure gradient caused by the gap flow. At all gaps the mean force on the cylinder was such as to repel it from the wall.

The flow round a cylinder near to a wall has been considered to be analogous to the flow around two cylinders in a side-by-side arrangement. For values of G/D above

about 0·5 the two flows are found to be similar. The flow about two cylinders becomes bistable for $G/D < 0{\cdot}5$ whereas a cylinder near a wall shows no such gross unsteadiness.

The most fascinating feature of our measurements of the flow around a circular cylinder near to a wall is the constancy of the Strouhal number as the gap is reduced even though the drag, base pressure and separation position change.

One of the authors (MMZ) would like to express his gratitude to Professor J. L. Livesey, former Head of the Department of Aeronautical and Mechanical Engineering, University of Salford, for making sabbatical leave at Imperial College (1976/77) possible, and to Professor P. R. Owen, Head of the Department of Aeronautics at Imperial College, for his hospitality during MMZ's stay.

REFERENCES

BEARMAN, P. W. & WADCOCK, A. J. 1973 The interaction between a pair of circular cylinders normal to a stream. *J. Fluid Mech.* **61**, 495–511.

BLOOR, S. 1964 The transition to turbulence in the wake of a circular cylinder. *J. Fluid Mech.* **19**, 290–304.

BROWN, G. L. & ROSHKO, A. 1974 On density effects and large structure in turbulent mixing layers. *J. Fluid Mech.* **64**, 775–816.

DAVIES, M. E. 1974 Spectral analysis programs Powspec and Cophase. *Imperial Coll. Aero. Tech. Note* no. 74–103.

GÖKTUN, S. 1975 The drag and lift characteristics of a cylinder placed near a plane surface. M.Sc. thesis, Naval Postgraduate School, Monterey, California.

QUADFLIEG, H. 1977 Wirbelinduzierte Belastungen eines Zylinderpaares in inkompressibler Strömung bei grossen Reynoldszahlen. *Forsch. Ing.-Wesen* **43**, 9–18.

ROSHKO, A., STEINOLFSON, A. & CHATTOORGOON, V. 1975 Flow forces on a cylinder near a wall or near another cylinder. *Proc. 2nd US Conf. Wind Engng Res., Fort Collins*, paper IV–15.

TANEDA, S. 1965 Experimental investigation of vortex streets. *J. Phys. Soc. Japan* **20**, 1714–1721.

ZDRAVKOVICH, M. M. 1977 Review of flow interference between two circular cylinders in various arrangements. *Trans. A.S.M.E., J. Fluids Engng* **99**, 618–633.

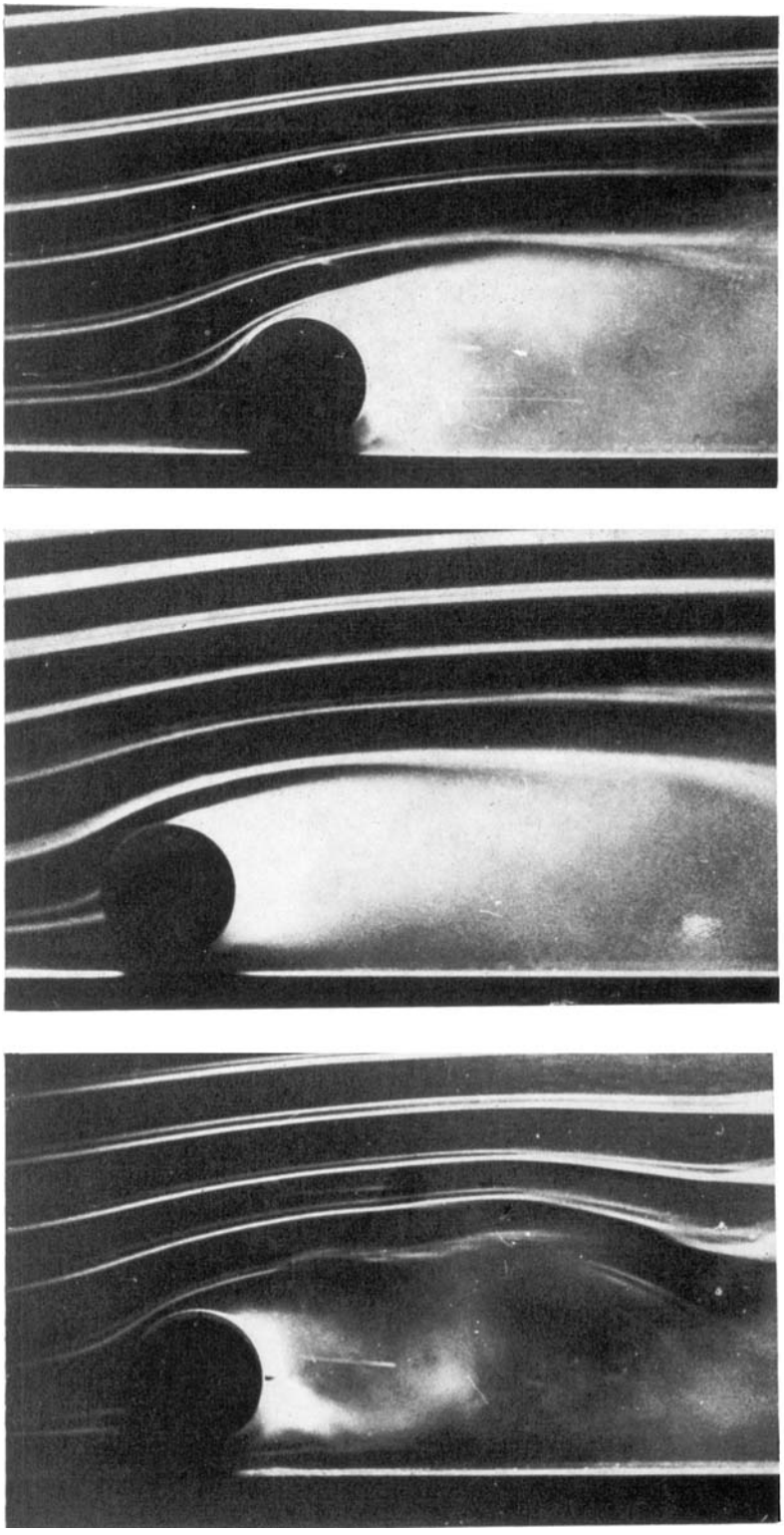

FIGURE 6. Flow pattern at $Re = 2{\cdot}5 \times 10^4$ ($L/D = 1$).
(*a*) $G/D = 0$; (*b*) $G/D = 0{\cdot}2$; (*c*) $G/D = 0{\cdot}4$.

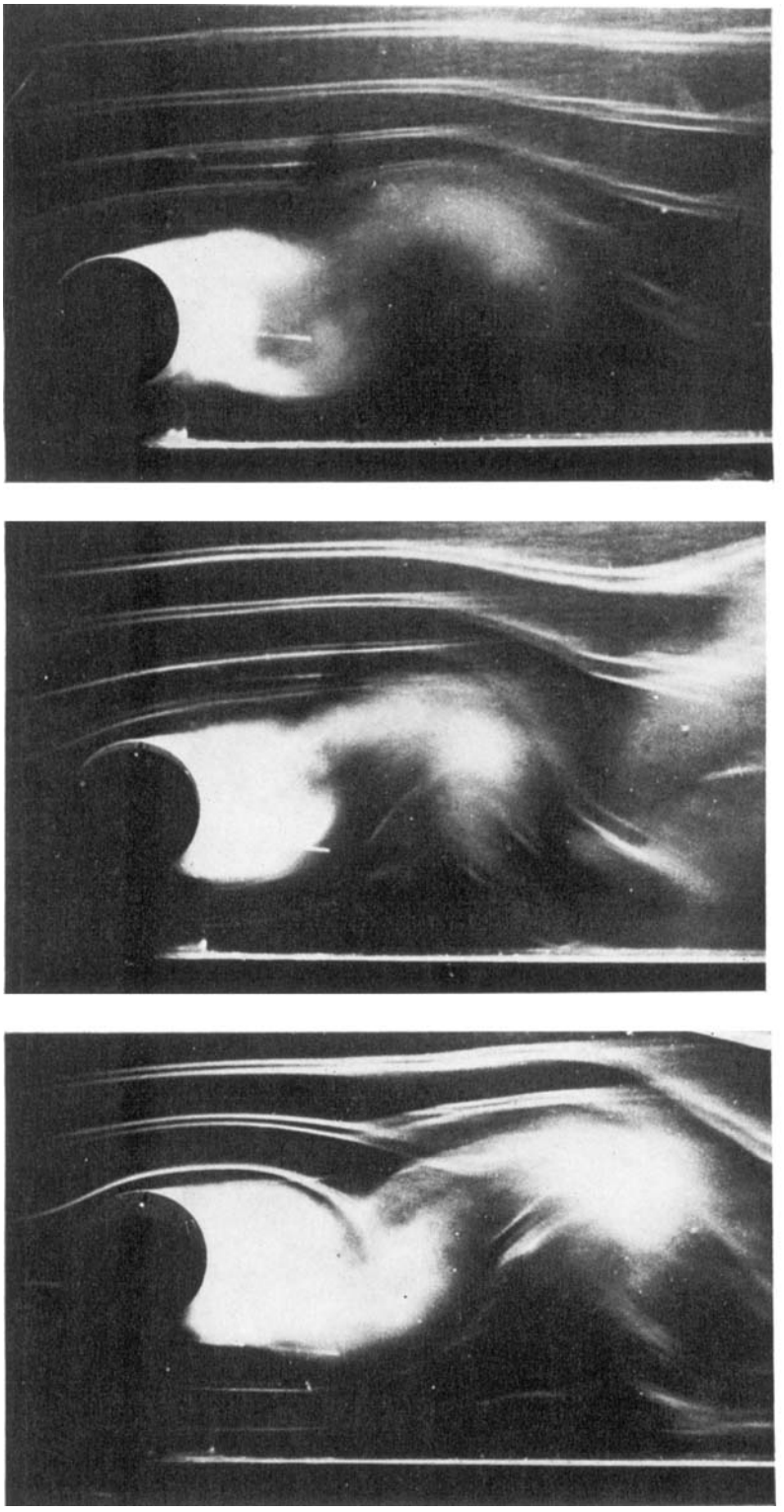

FIGURE 7. Flow pattern at $Re = 2{\cdot}5 \times 10^4$ ($L/D = 1$).
(*a*) $G/D = 0{\cdot}8$; (*b*) $G/D = 1{\cdot}2$; (*c*) $G/D = 2{\cdot}0$.

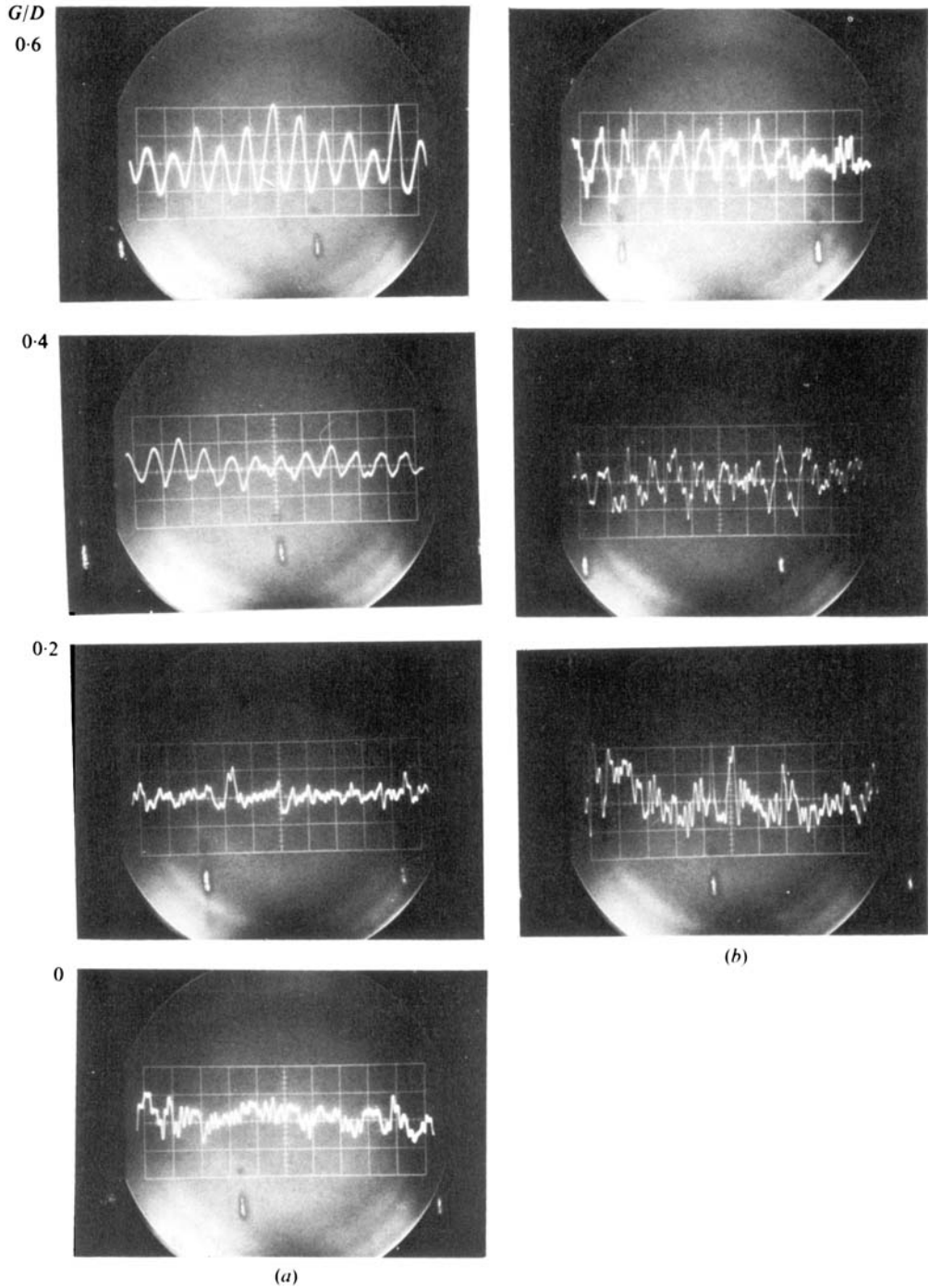

FIGURE 8. Oscillograms of velocity fluctuations detected by the hot wire positioned (*a*) near the upper edge of the wake and (*b*) near the lower edge of the wake.